ADVANCING EARTH AND SPACE SCIENCES

JGR Atmospheres

RESEARCH ARTICLE
10.1029/2023JD038761

Compounding Heatwave-Extreme Rainfall Events Driven by Fronts, High Moisture, and Atmospheric Instability

Christoph Sauter[1], **Jennifer L. Catto**[2], **Hayley J. Fowler**[3,4], **Seth Westra**[5], and **Christopher J. White**[1]

[1]Department of Civil and Environmental Engineering, University of Strathclyde, Glasgow, UK, [2]Department of Mathematics and Statistics, Faculty of Environment, Science and Economy, University of Exeter, Exeter, UK, [3]School of Engineering, Newcastle University, Newcastle, UK, [4]Tyndall Centre for Climate Research, Newcastle University, Newcastle, UK, [5]School of Civil, Environmental and Mining Engineering, University of Adelaide, Adelaide, SA, Australia

Key Points:

- The transition from heatwaves to extreme rainfall is usually associated with fronts and/or thunderstorm conditions
- Atmospheric instability and moisture are larger than during non-heatwave conditions and increase over several days before the termination
- Availability of moisture is important for producing extreme rainfall after heatwaves and explains the spatial variability for this event

Supporting Information:

Supporting Information may be found in the online version of this article.

Correspondence to:

C. Sauter,
christoph.sauter@strath.ac.uk

Citation:

Sauter, C., Catto, J. L., Fowler, H. J., Westra, S., & White, C. J. (2023). Compounding heatwave-extreme rainfall events driven by fronts, high moisture, and atmospheric instability. *Journal of Geophysical Research: Atmospheres*, *128*, e2023JD038761. https://doi.org/10.1029/2023JD038761

Received 23 FEB 2023
Accepted 20 SEP 2023

Author Contributions:

Conceptualization: Christoph Sauter, Jennifer L. Catto, Hayley J. Fowler, Seth Westra, Christopher J. White
Data curation: Jennifer L. Catto
Formal analysis: Christoph Sauter
Funding acquisition: Christopher J. White
Visualization: Christoph Sauter
Writing – original draft: Christoph Sauter
Writing – review & editing: Christoph Sauter, Jennifer L. Catto, Hayley J. Fowler, Seth Westra, Christopher J. White

Abstract

Heatwaves have been shown to increase the likelihood and intensity of extreme rainfall occurring immediately afterward, potentially leading to increased flood risk. However, the exact mechanisms connecting heatwaves to extreme rainfall remain poorly understood. In this study, we use weather type data sets for Australia and Europe to identify weather patterns, including fronts, cyclones, and thunderstorm conditions, associated with heatwave terminations and following extreme rainfall events. We further analyze, using reanalysis data, how atmospheric instability and moisture availability change before and after the heatwave termination depending on whether the heatwave is followed by extreme rainfall, as well as the location of the heatwave. We find that most heatwaves terminate during thunderstorm and/or frontal conditions. Additionally, atmospheric instability and moisture availability increase several days before the heatwave termination; but only if heatwaves are followed by extreme rainfall. We also find that atmospheric instability and moisture after a heatwave are significantly higher than expected from climatology for the same time of the year, and that highest values of instability and moisture are associated with highest post-heatwave rainfall intensities. We conclude that the joint presence of high atmospheric instability, moisture, as well as frontal systems are likely to explain why rainfall is generally more extreme and likely after heatwaves, as well as why this compound hazard is mainly found in the non-arid mid and high latitudes. An improved understanding of the drivers of these compound events will help assess potential changing impacts in the future.

Plain Language Summary

Extreme rainfall which can lead to flash floods is more likely to occur if it is preceded by a heatwave. The exact reasons behind this connection, however, are not fully clear. In this study we investigate the mechanistic drivers connecting heatwaves to extreme rainfall in Europe and Australia by analyzing which types of weather (e.g., fronts, cyclones, thunderstorms) are present during the transition from heatwaves to extreme rainfall. We also analyze how atmospheric characteristics associated with extreme rainfall during thunderstorms change depending on if a heatwave is followed by extreme rainfall or not. We find that heatwaves are usually followed by extreme rainfall when there are thunderstorm conditions and/or when there is the presence of a front. Further, we find that high amounts of moisture are present if heatwaves are followed by extreme rainfall and that atmospheric conditions favorable for thunderstorms, including high amounts of moisture are generally increased after heatwaves. These findings help understand how heatwaves are connected to extreme rainfall and can help assess how the risk from these events might change in the future.

1. Introduction

Short-duration extreme rainfall has the potential to cause severe flooding and is projected to increase in intensity as well as frequency as a result of anthropogenic climate change (Fowler et al., 2021; Prein et al., 2016; Seneviratne et al., 2021). One of the reasons for this projected increase is the thermodynamic connection between temperature and precipitable water in the atmosphere, since hotter air can hold more moisture (Trenberth et al., 2003). Heatwaves, where high temperatures persist over several days, usually coincide with dry weather due to land-atmosphere interactions (Miralles et al., 2019). While rainfall is therefore less likely *during* a heatwave, recent studies have shown a significant increase in extreme rainfall immediately *after* a heatwave (Chen et al., 2022; Li et al., 2022; Ning et al., 2022; Sauter et al., 2022; You & Wang, 2021). Heatwaves followed by extreme rainfall

10.1029/2023JD038761

should thus be seen as a compound event (Leonard et al., 2014; Zscheischler et al., 2018), as the likelihood and intensity of the extreme rainfall event is increased compared to conditions without a heatwave.

This compounding hot-wet extreme event occurs predominately in the mid and high latitudes where there is ample moisture supply and high summer temperatures (Sauter et al., 2023). Several studies therefore point toward moist convection being the main driver of compounding heatwave-extreme rainfall events, as atmospheric instability tends to be high during the event (Chen et al., 2022; Wu et al., 2021; You & Wang, 2021; Zhang & Villarini, 2020). Indeed, from a theoretical standpoint, high temperatures related to the heatwave have the potential to enhance convective extreme rainfall, provided there is ample moisture supply, as extreme rainfall associated with convection is usually linked to high atmospheric instability and moisture (Brooks, 2013; Groenemeijer & Van Delden, 2007; Meyer et al., 2022; Púčik et al., 2015). However, uncertainties remain as to how other synoptic-scale drivers contribute; cyclones or fronts could be the causal mechanism of both the reduction in ambient temperature during the heatwave termination as well as the associated rainfall. Further, it is unclear if the low likelihood of extreme rainfall after heatwaves in arid regions results from the absence of synoptic systems associated with rainfall, a lack of available moisture and atmospheric instability, or both.

Identifying convective- and synoptic-scale drivers for extreme events such as extreme rainfall is challenging as the drivers are identified using different atmospheric variables and methods. Recent studies have addressed this by identifying weather types such as thunderstorms, fronts, and cyclones that can also occur simultaneously in space and time (Catto & Dowdy, 2021; Dowdy & Catto, 2017; Pepler et al., 2020). Therefore commonly known drivers of extreme rainfall in Australia and Europe, such as east coast lows, tropical and extratropical cyclones, fronts, atmospheric rivers and/or thunderstorms (Catto & Pfahl, 2013; Dowdy & Catto, 2017; Dowdy et al., 2019; Lavers & Villarini, 2013; Villarini & Denniston, 2016), can be easily identified and causally related to an extreme event.

Here, we determine the predominant weather-types during heatwave terminations in Australia and Europe, giving insight into the importance of convective and synoptic-scale drivers of extreme rainfall following heatwaves. We further investigate how and why the strength of this compound event differs by region. Improved understanding of the driving mechanisms is crucial to estimating future changes to extreme rainfall after heatwaves and the resulting potential impacts.

2. Data

The selection of rainfall and temperature data, as well as the definition of heatwaves follows that of previous work (Sauter et al., 2022) where different definitions and thresholds have been tested and found not to impact results significantly. Due to the availability of weather type data sets in these regions, the analysis focusses on Europe and Australia.

2.1. Rainfall Observations

We use hourly rainfall observations from the Global Sub-Daily Rainfall Dataset (GSDR) (Lewis et al., 2019a) which have been extensively quality-controlled (Ali et al., 2022; Lewis et al., 2021). Here, we only consider stations with at least 12 years of rainfall records and less than 20% of missing data during any year (analog to Ali et al. (2021)). As rainfall observations are paired up with temperature data as well as with weather type data, rainfall records are limited to starting from 1979 or later. This results in the analysis of 1987 stations in Europe and 581 stations in Australia. Extreme rainfall is defined for each station individually as an hourly rainfall event that exceeds the respective 99th percentile of all hours with >0.1 mm/hr within the entire rainfall record. This ensures that the 99th percentile rainfall threshold is higher than if using the 99th percentile of wet and dry hours, as excluding non-rainfall hours reduces the number of values and extreme values vary less between locations depending on the respective climatological number of dry days/hours per year.

2.2. Reanalysis Data

We additionally use 2-m temperature, total column water vapor (TCWV), and convective available potential energy (CAPE) variables from the ERA5 reanalysis data set (Hersbach et al., 2020). The data is provided at a horizontal resolution of 31 km and the grid box closest to each GSDR station is selected. All variables are aggregated from hourly to daily timescales with respect to their local time zones (maximum and minimum daily temperatures; T_{max}, T_{min}, mean daily TCWV and CAPE). Other variables describing moisture (e.g., absolute humidity) and atmospheric instability (e.g., convective inhibition) are available from reanalysis as well; however, TCWV and CAPE are analyzed as they have been found to serve well as proxy parameters for conditions associated with extreme precipitation (Meyer et al., 2022).

2.3. Weather Type Data

We use two weather type data sets that cover Europe and Australia respectively. For Europe we use a weather type data set following Dowdy and Catto (2017) and Catto and Dowdy (2021) that determines cyclones, fronts, and thunderstorms from ERA5 data. The fronts are identified using an updated version of a thermal front parameter method (Sansom & Catto, 2022), and the cyclones are identified using the Wernli and Schwierz (2006) method of identifying closed contours of mean sea level pressure. The thunderstorm environment is defined using CAPE, bulk wind shear from 0 to 6 km, total totals index and a Laplacian of 500-hPa geopotential height (Dowdy & Brown, 2023) and the thresholds are based on lightning observations (Dowdy, 2020). The individual weather systems can occur by themselves or in combination with other systems. Therefore, the combination of these three identified systems means that the weather types included in the Europe region are Cyclone Only (CO), Front Only (FO), Thunderstorm Only (TO), Cyclone-Front (CF), Cyclone-Thunderstorm (CT), Front-Thunderstorm (FT), Cyclone-Front-Thunderstorm (CFT), and Undefined (U). The data set is provided at 0.25° resolution, spanning 1980 to 2019.

For Australia, we use a weather types data set from Pepler et al. (2020), based on the ERA-Interim reanalysis, which follows Dowdy and Catto (2017) but includes a number of additional identification algorithms. In this data set, fronts are identified using both the thermal front parameter method (Berry et al., 2011; Hewson, 1998), and a wind shift method (Simmonds et al., 2012). Cyclones are identified using mean sea level pressure with both the Wernli and Schwierz (2006) method and the University of Melbourne algorithm (Murray & Simmonds, 1991; Simmonds & Keay, 2000; Simmonds et al., 1999). If a front or cyclone is only identified with one of their respective two identification methods, they are classified as "Unconfirmed Cyclones/Fronts (UCF)." More detailed information about the identification of each individual weather system can be found in Pepler et al. (2020). For any given time and location, if none of the previous weather types is identified, the weather type at that location is "Undefined" ("*U*"). Therefore, in addition to the eight weather types used in Europe, three additional weather types are included for Australia: High pressure (*H*), Warm-front (WF), "Unconfirmed Cyclones/Fronts (UFC)." The data set for Australia is provided at a gridded 0.75° horizontal resolution from 1979 to 2015. For each GSDR station the corresponding grid box from the European or Australian weather type data set are selected.

3. Methods

Heatwaves are defined for each location individually, where T_{max} lies above its 95th percentile for at least 3 consecutive days and T_{min} lies above its 95th percentile for at least the second and third day. To avoid a longer heatwave being identified as two or more shorter heatwaves, a heatwave is only terminated if T_{max}, T_{min}, or a combination of the two, fall below their respective thresholds for at least two consecutive days. The robustness of the heatwave-extreme rainfall signal has also been tested for different heatwaves definitions and thresholds in a previous study (Sauter et al., 2022), and these were not found to change the results significantly. However, to test the influence of different heatwave types on available moisture, we define day-time heatwaves as a minimum of three consecutive days where T_{max} lies above its 95th percentile, while T_{min} lies below its 95th percentile during the same days. Analog to this definition, we define night-time heatwaves as a minimum of three consecutive days where T_{min} lies above its 95th percentile, while T_{max} lies below its 95th percentile during the same days.

To avoid identifying localized reductions in temperature as large-scale heatwave terminations, we only consider heatwave terminations where at least two stations agree on the timing of a termination. We found that requiring more stations does not significantly change the results, and therefore use two stations as a minimum to increase the number of identified heatwaves. For each heatwave termination, we select the weather type that is present at most of the affected stations at the termination. Weather type distributions are analyzed at 12:00 on the last day of the heatwave. The distribution of weather types for different times throughout and after the heatwave is shown in Figures S1 and S2 of the Supporting Information S1. For CAPE and TCWV, we calculate the station-mean of all affected stations.

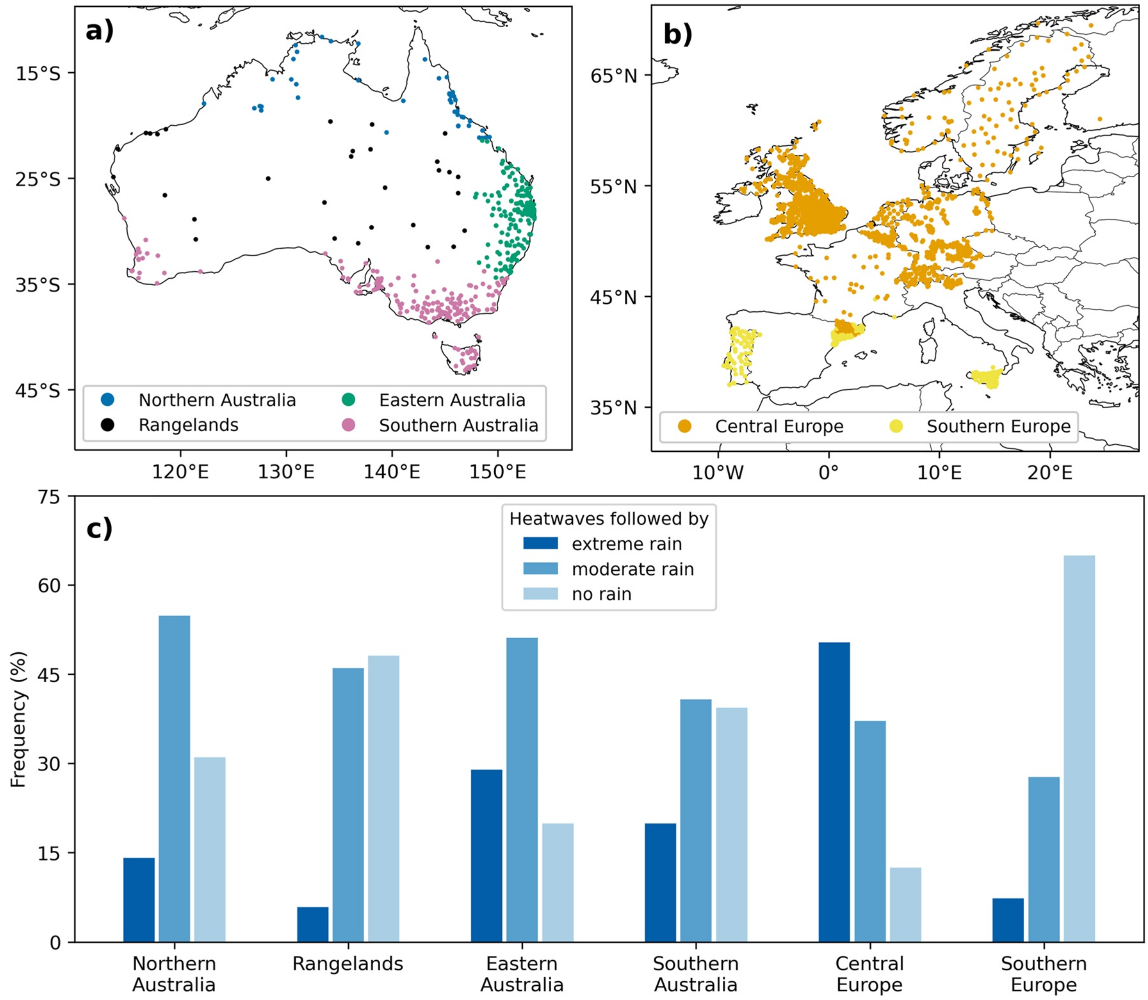

Figure 1. Location of rainfall stations used for Australia (a) and Europe (b). The stations are colored according to their region used in this study (44 in Northern Australia, 165 in Eastern Australia, 30 in Rangelands, 186 in Southern Australia, 1479 in Central Europe and 227 in Southern Europe). (c) Percentage of heatwaves ending with extreme rainfall (dark blue), moderate rainfall (blue), or no rainfall (light blue) for each of the regions used within Australia and Europe.

The influence of a heatwave on the likelihood and intensity of extreme rainfall is strongest immediately (24–48 hr) after a heatwave (Chen et al., 2022; Sauter et al., 2022). We therefore consider any rainfall connected to a heatwave termination if it occurs within a 36-hr time window starting on noon on the last day of a heatwave. Though the signal of a heatwave on subsequent rainfall can last up to several days, the strongest rainfall response occurs within the first day after a heatwave (Chen et al., 2022; Sauter et al., 2022).

All heatwave terminations are then divided further into three categories based on the rainfall following the heatwave:

(1) *Heatwaves followed by extreme rainfall*; At least one station records at least 1 hr of extreme rainfall after the heatwave.
(2) *Heatwaves followed by moderate rainfall*; At least one station records at least one wet hour (>0.1 mm/hr) after the heatwave, but none of the stations record any extreme rainfall.
(3) *Heatwaves followed by no rainfall*; No station records any rainfall after a heatwave.

Figure 1 shows the location of GSDR stations used for this study in Australia (a) and Europe (b). Stations in Australia and Europe have been sub-divided to account for differences in climatic conditions. Australia is sub-divided into four (Northern Australia, Rangelands, Eastern Australia and Southern Australia) according to the regions suggested by CSIRO and Bureau of Meteorology (2015). Europe has been divided into two; Central Europe and Southern Europe, based on Köppen-Geiger climate classifications (Beck et al., 2018). Central

10.1029/2023JD038761

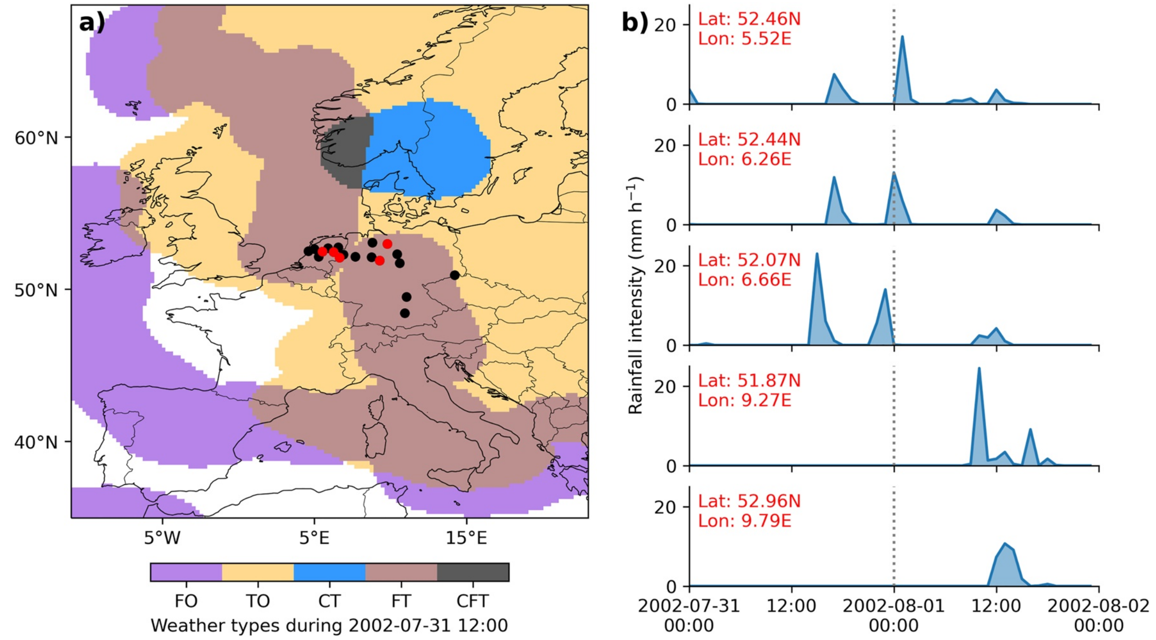

Figure 2. Case study of a heatwave termination with extreme rainfall on the 31 July 2002 in Central Europe. (a) Shadings show areas associated with a particular weather type during 12:00 on the last day of the heatwave. Dots indicate locations of all stations where a heatwave terminates on the 31 July 2002. Red dots indicate locations of the five stations with the highest recoded hourly rainfall of all stations affected by the heatwave termination, and their observed rainfall intensity is shown in (b), ordered from east to west (top to bottom in (b)). Vertical dashed lines indicate the end of the heatwave.

Europe includes Moderate, Cold, and Polar climate classifications that are associated with high likelihoods of extreme rainfall after heatwaves (Köppen-Geiger sub-classes "Cfa," "Cfb," "Cfc," "Dfb," "Dfc," and "ET"), and Southern Europe contains Arid and Moderate climate classifications associated with low likelihoods of extreme rainfall after heatwaves (Köppen-Geiger sub-classes "BSk," "Csa," and "Csb") (Sauter et al., 2023). All major Köppen-Geiger climate classifications (Tropical, Arid, Moderate, Cold and Polar) are represented within at least one of the six regions.

Figure 1c shows that the likelihood of (extreme) rainfall after a heatwave varies depending on the region and climatic conditions. In Australia, extreme rainfall after heatwaves is most likely in Eastern Australia, followed by Southern Australia, while heatwaves in Northern Australia and the Rangelands are less likely to be followed by extreme rainfall. In Europe, heatwaves are far more likely to be followed by extreme rainfall in Central Europe than in Southern Europe.

To estimate the frequency of a particular weather type and atmospheric conditions such as TCWV and CAPE independent of any heatwave occurrence, we calculate climatological estimations for weather type frequencies, TCWV and CAPE for the same time of the year as the heatwave. For each heatwave termination (i.e., all stations whose heatwave ended on the same day), we calculate the weather type, TCWV and CAPE for the same day of the year for all available years in the respective record. If a heatwave termination falls on the last day of a year during a leap year, as in some instances in Australia, the 365th instead of the 366th day of the year is chosen in order not to reduce the sample size.

4. Results

During any given time, multiple weather types can be present in one region, as illustrated in a case study example from a heatwave termination followed by extreme rainfall in summer 2002 (Figure 2). During this heatwave termination, most of Europe was under a thunderstorm environment. The termination of the heatwave and associated extreme rainfall, however, was associated with the passage of a front. Though part of the same frontal structure, the weather types data set allows separating frontal conditions that occur simultaneously with and without thunderstorm conditions (brown and purple areas, respectively). During the 36-hr window from 12:00 on the last heatwave day, 16 of the 23 stations with heatwave terminations on that day recorded at least 1 hr of extreme rainfall.

10.1029/2023JD038761

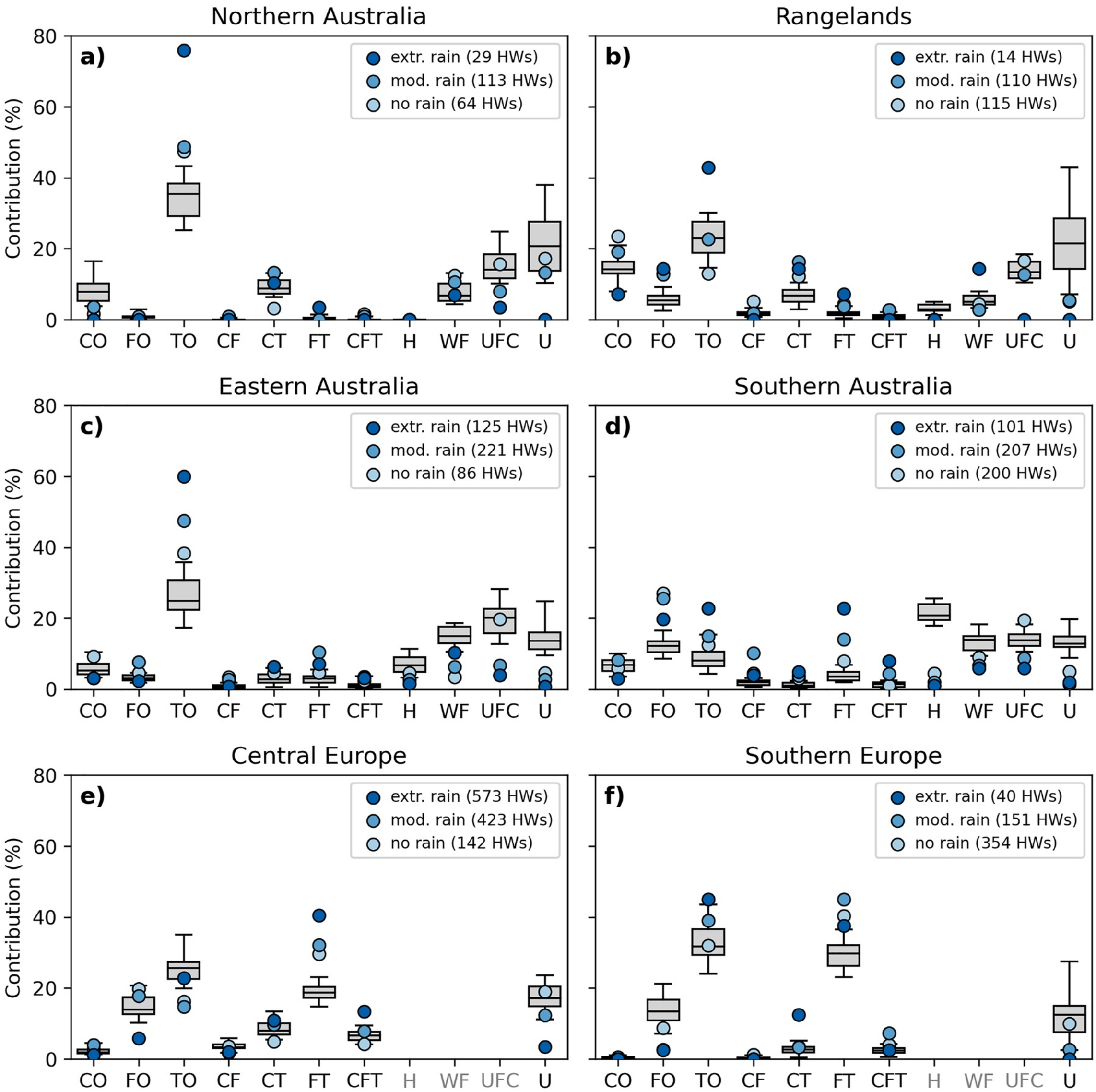

Figure 3. Frequency of each weather type at 12:00 on the last day of a heatwave for heatwaves followed by extreme rain (dark blue dots), moderate rain (blue dots) or no rain (light blue dots) for Northern Australia (a), Rangelands (b), Eastern Australia (c), Southern Australia (d), Central Europe (e), and Southern Europe (f). Gray boxplots show climatological distribution of weather types during the same time of the year as the heatwaves and whiskers extend from the 5th to 95th percentile. The number in brackets in the legends show number of heatwaves identified for each of the three heatwave endings in the respective region. The weather types High (H), Warm-front (WF), and Unconfirmed Fronts/Cyclones (UFC) are only available for Australia.

Heatwaves in Europe and Australia tend to terminate during frontal (F) and/or thunderstorm (T) conditions (Figure 3). While these weather types are also very common climatologically, there were statistically significant differences between the frequency of particular weather types during heatwave terminations and climatology. In all regions (except Central Europe), Thunderstorm Only conditions occurred significantly more often than expected from climatology (i.e., above the 95th percentile) in cases where a heatwave was followed by extreme rainfall. If a heatwave in the same regions was followed only by moderate or no rainfall, Thunderstorm Only conditions were mostly more likely than or comparable to conditions expected from climatology. Significantly higher Front Only conditions during all heatwave termination types compared to climatology were found in the Rangelands and Southern Australia but were comparable or less likely than climatology in the other regions. The combination of fronts and thunderstorms were significantly more likely than climatology during all heatwave endings in Southern Australia and Central Europe, but the signal is less clear in the other regions and dependent on the type of heatwave termination. There is some indication that Cyclone-Front-Thunderstorm conditions during heatwave terminations were also more likely than climatology in the Rangelands, Eastern Australia, Southern Australia, and Southern Europe. However, the absolute occurrences were comparably low and the difference to climatology is only significant for certain heatwave termination types such as heatwaves followed by extreme rainfall in Southern Australia or Central Europe. Cyclone Only weather type occurrences during heatwave terminations were usually not significantly different to climatology, except for the Rangelands, where heatwaves followed by no rain were associated with Cyclone Only conditions significantly more often than expected from climatology. Cyclone-Thunderstorm weather types during heatwaves mostly made up only a small contribution overall and were mostly comparable to climatology, with the exception of the Rangelands where Cyclone-Thunderstorm weather types were significantly more likely than climatology during all heatwave endings. High, Warm-front, and Unconfirmed Fronts/Cyclones weather types tended to be less frequent during heatwave terminations than climatology (often significantly less frequent, e.g., in Southern Australia), though there were some exceptions like in the Rangelands, where a significantly higher contribution of WF weather types compared to climatology occurred during heatwave terminations which were followed by extreme rainfall. The proportion of undefined (U) weather types was lower than expected from climatologic conditions during all heatwave terminations. Overall, weather types related to thunderstorms and fronts (i.e., Thunderstorm Only, Front Only, and Front-Thunderstorm) tended to be more likely during heatwave terminations, especially if a heatwave was followed by extreme rainfall.

The weather type analysis shows that the likelihood of a specific weather type during heatwave termination varies by region, but much less by whether a heatwave is followed by (extreme) rainfall and cannot fully explain why some heatwaves are followed by extreme rainfall while others in the same region are not. We therefore analyze if these differences in rainfall behavior after heatwaves can be explained by variations in atmospheric conditions. Specifically, we analyze the atmospheric instability and availability of moisture before and after the heatwave termination as these are important requirements for extreme rainfall in thunderstorms and their mechanistic roles in contributing to extreme rainfall is well known (Meyer et al., 2022).

Figure 4 shows convective available potential energy (CAPE) and total column water vapor (TCWV) for Australia and Europe during and after a heatwave conditional on whether the heatwave was followed by extreme, moderate, or no rainfall. In all the regions studied in Australia and Europe, if a heatwave is followed by extreme rainfall, CAPE increases during the heatwave until the last day or the day after the heatwave. However, the duration of the buildup in CAPE varies from only one or 2 days in the Rangelands or Southern Europe, to several days in the other regions. For a heatwave followed by only moderate rainfall, CAPE also increases, but at a lower magnitude. In contrast, a heatwave followed by no rainfall shows little to no increase in CAPE.

TCWV shows a similar behavior. A heatwave followed by extreme rainfall shows a strong increase in TCWV in the lead up to heatwave termination. TCWV values tend to peak on the first day after termination (except in Central Europe where the peak occurs on the last heatwave day) and are not necessarily linked with the peak in CAPE. A heatwave followed by moderate rainfall shows similar increases in TCWV, but at a lower magnitude. TCWV remains low for a heatwave followed by no rainfall.

CAPE, and to a lesser degree TCWV, also vary depending on the present weather type during a heatwave termination, as demonstrated here for Southern Australia (Figure 5). During thunderstorm conditions (Thunderstorm Only and Front-Thunderstorm), both CAPE and TCWV show high values during a heatwave termination if a heatwave is followed by extreme rainfall. This is unsurprising, as CAPE is one of the two parameters used to determine the thunderstorm weather type (Section 2.3). CAPE during the Front-Thunderstorm weather type is lower than during the Thunderstorm-Only conditions. Heatwaves terminations associated with frontal conditions alone are associated with much lower values of CAPE. TCWV, however, remains high during both frontal and thunderstorm-related weather types. The highest values of TCWV and CAPE are still found in cases where a heatwave is followed by extreme rainfall and are lower where a heatwave is followed by moderate or no rainfall. Similar behaviors can be found in the other regions as well (Figures S3–S7 in Supporting Information S1).

TCWV and CAPE on the last day the heatwave are also strongly related to the maximum 1 hr rainfall intensity after heatwave termination (Figure 6). The maximum 1 h rainfall intensities are calculated as the highest hourly rainfall recorded at any station affected by the heatwave termination within 36 hr of 12:00 on the last heatwave day. In all regions, the highest rainfall events are also associated with high values of TCWV and CAPE for the respective region. Lower rainfall maxima are associated with lower TCWV and CAPE values. Heatwaves that terminate without rainfall also tend to have noticeably lower values of TCWV and CAPE. Dry regions such as Rangelands or Southern Europe produce high values of CAPE; however, TCWV is comparably low, especially

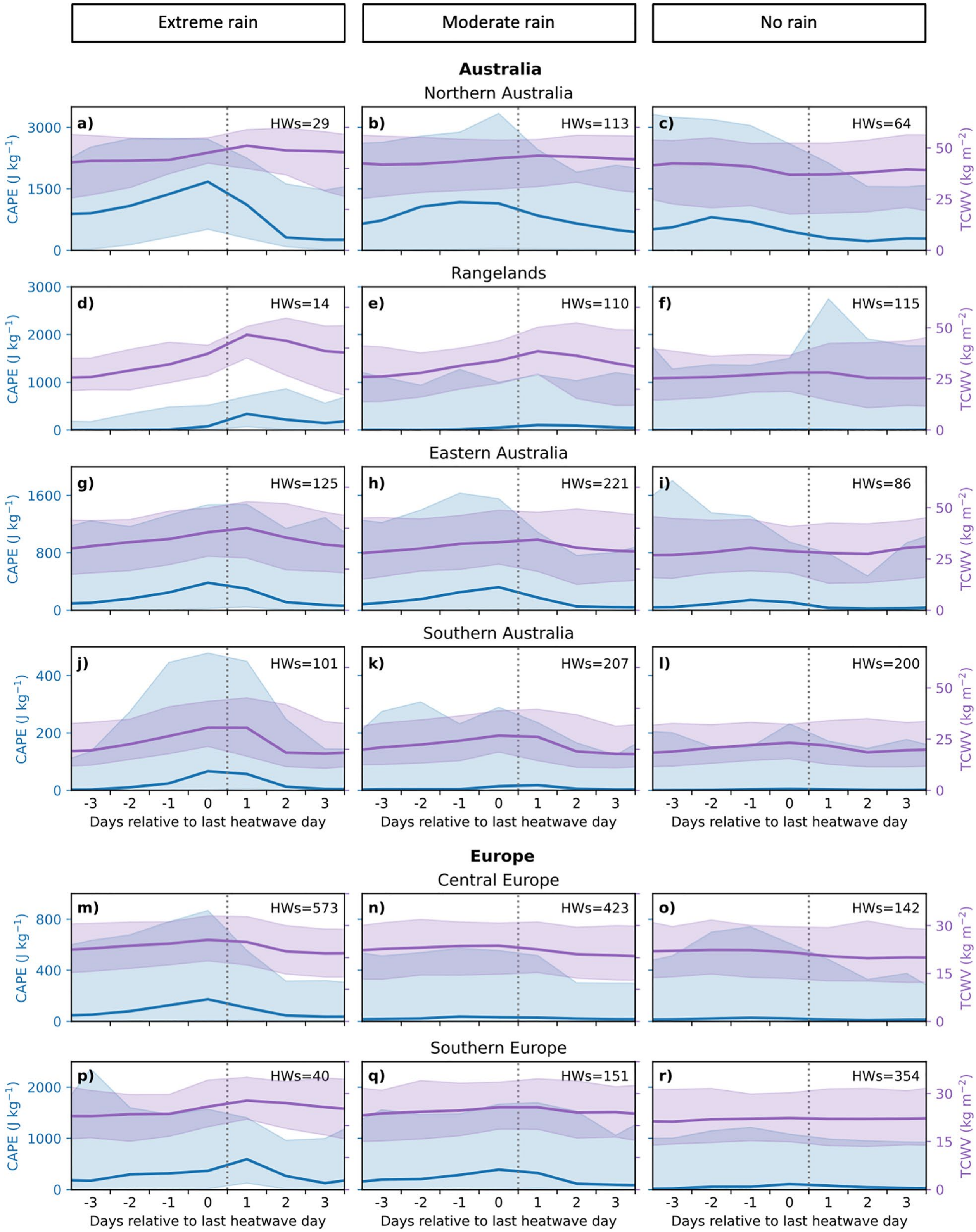
Extreme rain
Moderate rain
No rain
Australia
Northern Australia
a) HWs=29
b) HWs=113
c) HWs=64
Rangelands
d) HWs=14
e) HWs=110
f) HWs=115
Eastern Australia
g) HWs=125
h) HWs=221
i) HWs=86
Southern Australia
j) HWs=101
k) HWs=207
l) HWs=200
Europe
Central Europe
m) HWs=573
n) HWs=423
o) HWs=142
Southern Europe
p) HWs=40
q) HWs=151
r) HWs=354
CAPE (J kg⁻¹)
TCWV (kg m⁻²)
Days relative to last heatwave day

Figure 4.

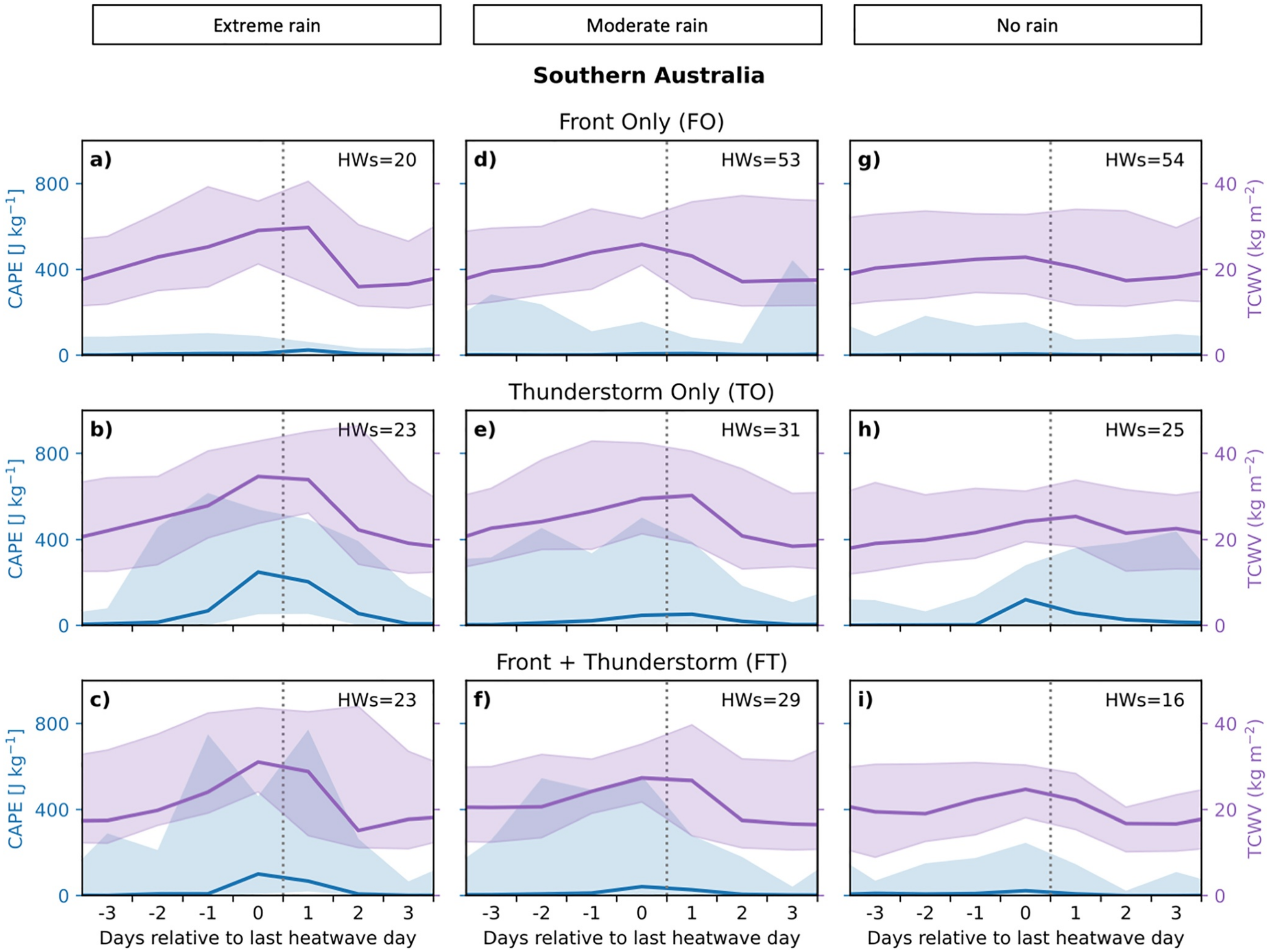

Figure 5. Like Figure 4, but for Southern Australia and showing heatwaves for the three most common weather types associated with heatwaves followed by extreme rainfall. Top row (middle row, bottom row) shows CAPE and TCWV during and after heatwaves if the dominant weather type during the heatwave termination at 12:00 was Front Only (FO) (Thunderstorm Only; TO, Front-Thunderstorm; FT). The other regions are shown in Figures S3–S7 of the Supporting Information S1.

for dry heatwave termination. In moderate climates such as Eastern Australia or Central Europe, high CAPE values are more strongly associated with high rainfall. The same relationship between CAPE, TCWV and 1 hr extreme rainfall can also be seen for CAPE and TCWV values on the day after a heatwave termination (Figure S8 in Supporting Information S1).

To further investigate the influence of the heatwave on rainfall production, we compare distributions of TCWV and CAPE on the last day of the heatwave to climatology (Figure 7). TCWV on the last day of a heatwave is significantly higher ($p < 0.01$ with a Student's t-test) than expected from climatology for all regions except for Northern Australia. CAPE on the last day of the heatwave is also significantly higher ($p < 0.01$ with a Student's t-test) for all regions except for the Rangelands. Similar differences in CAPE and TCWV compared to climatology can also been seen on the day after the heatwave (Figure S9 in Supporting Information S1). We further find that night-time heatwaves are associated with a higher moisture increase during the heatwave termination compared to regular heatwaves (high temperatures during day and night, Figures S10 and S11 in Supporting

Figure 4. CAPE (blue) and TCWV (purple) during and after heatwaves for heatwave followed by extreme rain (left columns), moderate rain (center columns) or no rain (right columns). First four rows show CAPE and TCWV for four regions in Australia (Northern Australia, Rangelands, Eastern Australia, and Southern Australia; rows 1–4 respectively) and bottom two rows show CAPE and TCWV for two regions in Europe (Central Europe, and Southern Europe; rows 5–6, respectively). X-axis denotes the day relative to the last day of the respective heatwave. Solid lines show median values of CAPE and TCWV for each day relative to the heatwave and shading show the respective 5th–95th percentile ranges. Top right corner of each plot shows number of heatwaves identified for the respective region and heatwave ending. Vertical dashed lines indicate the end of the heatwave.

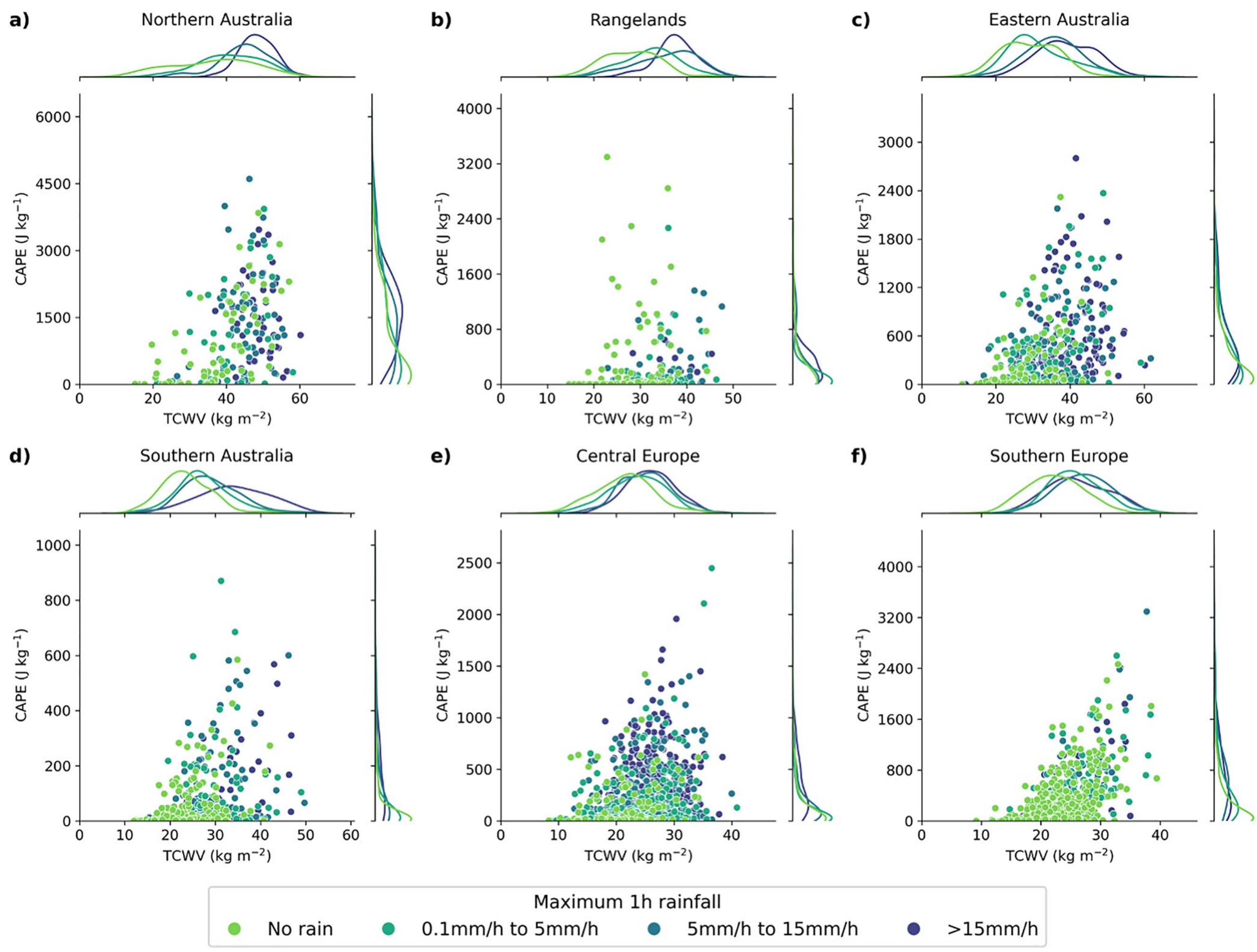

Figure 6. TCWV (*x*-axis) and CAPE (*y*-axis) for all stations on the last day of each heatwave for regions in Australia (a–d) and Europe (e–f). Data is separated by color by the maximum 1-hr rainfall of all stations experiencing a heatwave over a 36-hr period starting from 12:00 on the last heatwave day. The 1-hr rainfall maxima have been sorted into intensities of >15 mm/hr, 15–5 mm/hr, 5–0.1 mm/hr as well as no rainfall. Curves above (to the right of) the scatter plots show normalized kernel density estimates (estimated distributions) of TCWV (CAPE).

Information S1). Day-time heatwaves on the other hand show an increase in TCWV compared to climatology only in Southern Australia and Central Europe, while in all other regions TCWV during the heatwave termination is lower compared to climatology.

5. Discussion

We have demonstrated that heatwaves mostly terminate during thunderstorm and/or frontal conditions. Thunderstorm-related environments are generally more likely during the warmer months of the year (Dowdy, 2020), and high temperatures during heatwaves are likely to favor thunderstorm conditions by increasing atmospheric instability. During heatwave terminations, thunderstorm environments are more common in cases where a heatwave was followed by extreme rainfall compared to a heatwave followed by moderate or no rainfall. In these cases, the frequency of thunderstorm conditions is significantly higher than expected from climatology. While thunderstorms are potentially enhanced by the heatwave itself, fronts might occur more independently of the heatwave but are likely the cause the heatwave termination. Cold fronts are associated with the advection of cooler air—and thereby reduce the ambient temperature. However, it is important to note that from our analysis alone it is not possible to distinguish with certainty if heatwaves increase the likelihood of synoptic disturbances, synoptic disturbances contribute to the termination of the heatwave, or both. Besides their role in terminating heatwaves, fronts can also contribute to extreme rainfall by introduc-

10.1029/2023JD038761

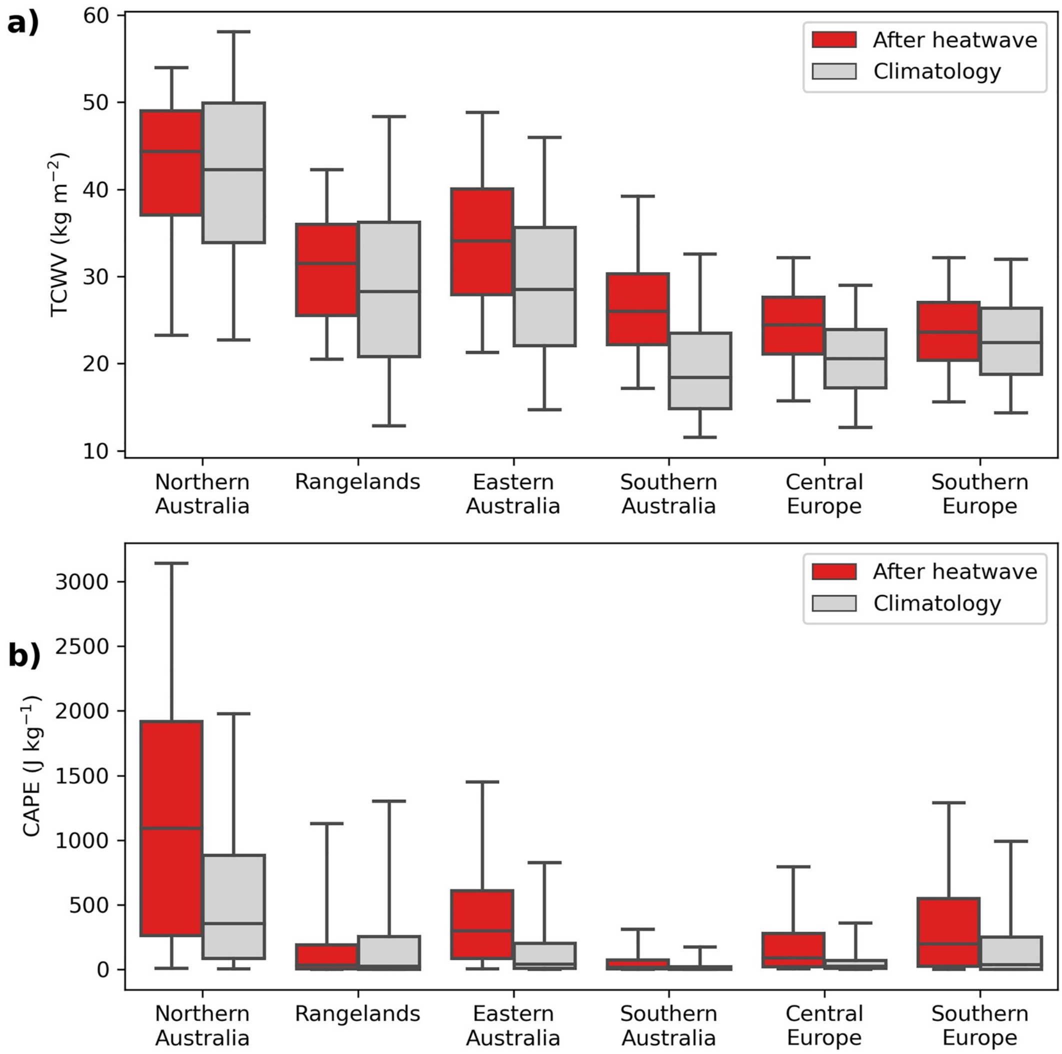

Figure 7. Distribution of TCWV (a) and CAPE (b) on the last day of the heatwave (red) and for climatology (gray) for the six regions used in this study. The boxplot whiskers extend from the 5th to 95th percentile.

ing further moisture as they are often associated with atmospheric rivers (Catto & Pfahl, 2013; Lavers & Villarini, 2013). Further, fronts could also act as a dynamical trigger of convection (e.g., Browning, 1986). As thunderstorm conditions are common during a heatwave termination (Figure 3), the combined occurrence with a front could therefore contribute to the observed higher rainfall intensities and likelihoods of extreme rainfall after heatwaves.

We further show that the likelihood and intensity of (extreme) rainfall after a heatwave is influenced by atmospheric instability and moisture availability. Both CAPE and TCWV are highest during terminations of heatwaves that are followed by extreme rainfall compared to heatwaves followed by moderate or no rainfall. We find that CAPE and TCWV vary depending on the weather type, with high values of CAPE only found during thunderstorm-related conditions. High values of TCWV were found in cases where a heatwave was followed by extreme rainfall regardless of the present weather type, indicating that high values of moisture are an essential condition for extreme rainfall after heatwaves. Other studies have also demonstrated high values of atmospheric instability (Chen et al., 2022; You & Wang, 2021; Zhang & Villarini, 2020) and moisture (Zhang & Villarini, 2020) during the transition from a hot to a wet extreme. Both CAPE and TCWV may increase due to the arrival of a frontal system and the associated advection of moisture. However, it is likely that the conditions during the heatwave also contribute, since the increase in both variables can be observed for several days before the heatwave termination, even during frontal conditions.

These results further explain why extreme rainfall following heatwaves as a compound extreme is far more likely in mid to high latitudes (Sauter et al., 2023) than elsewhere. Mid and high latitudes are usually characterized by moderate to polar climates with high temperatures and comparably high moisture availability during summer, providing good conditions for high atmospheric instability and moisture during heatwave terminations. In arid regions, however, as represented here by the Rangelands and Southern Europe regions, most heatwaves are not accompanied by increases in CAPE or TCWV (Figure 4). Additionally, frontal systems tend to occur more in higher latitudes, such as in Central Europe and Southern Australia, where both regions are characterized by high likelihoods of extreme rainfall after heatwaves.

Using station-based observations to detect rainfall improves the representation of extremes; however, this might lead to instances where small-scale rainfall after heatwaves is not detected. This would lead to heatwaves being falsely categorized as followed by moderate rainfall even though rainfall elsewhere was extreme, or as followed by no rainfall even though there was rainfall elsewhere. This is more likely in cases where heatwaves were only identified for a small number of stations. However, we have found that using a higher minimum number of stations does not change the results significantly, while reducing the available heatwave sample size.

6. Conclusions

In conclusion, we have shown that heatwave terminations in Australia and Europe are usually related to thunderstorm and/or frontal conditions. The likelihood of extreme rainfall occurring in the wake of a heatwave, however, is mainly governed by the atmospheric instability and moisture availability. The highest rainfall intensities after heatwaves are usually related to the highest values of atmospheric instability and moisture, which are in turn higher than without a heatwave. However, in the higher latitudes frontal systems are likely to contribute to the likelihood and intensity of extreme rainfall after heatwaves as well, as they can trigger convection and potentially introduce further moisture. Accurately estimating future changes to this compound event will therefore involve studying changes in both synoptic variability as well as the atmospheric parameters influencing convection.

Conflict of Interest

The authors declare no conflicts of interest relevant to this study.

Data Availability Statement

The publicly available subset of the GSDR observations can be obtained through Lewis et al. (2019b). ERA5 reanalysis data is available through Hersbach et al. (2020). The European weather type data set is available through Catto (2023). The Australian weather type data set is available through Pepler (2022). Shape files for the Australian regions are available through CSIRO and Bureau of Meteorology (2015). Köppen-Geiger maps which were used to define regions in Europe can be accessed through Beck et al. (2018).

Acknowledgments

C.S. was funded by an EPSRC Doctoral Training Partnership (DTP) (Grant EP/R513349/1). J.L.C and H.J.F. were supported by NERC project STORMY-WEATHER (Grant: NE/V004166/1). H.J.F. and C.J.W. were supported by the NERC Global Partnerships Seedcorn Fund (EMERGE; Grant: NE/W003775/1). H.J.F. was also supported by the United Kingdom NERC Changing Water Cycle programme (FUTURE-STORMS; Grant: NE/R01079X/1), and C.J.W. was supported by the Horizon Europe Multi-hazard and risk informed system for Enhanced local and regional Disaster risk management project (MEDiate; 10049641). This work used JASMIN, the UK's collaborative data analysis environment (https://jasmin.ac.uk) for post-processing ERA5 data. The authors would like to thank Acacia Pepler for providing the Australian weather type data set and Andrew Dowdy for providing the thunderstorm data for Europe.

References

Ali, H., Fowler, H. J., Lenderink, G., Lewis, E., & Pritchard, D. (2021). Consistent large-scale response of hourly extreme precipitation to temperature variation over land. *Geophysical Research Letters*, *48*(4), e2020GL090317. https://doi.org/10.1029/2020gl090317

Ali, H., Fowler, H. J., Pritchard, D., Lenderink, G., Blenkinsop, S., & Lewis, E. (2022). Towards quantifying the uncertainty in estimating observed scaling rates. *Geophysical Research Letters*, *49*(12), e2022GL099138. https://doi.org/10.1029/2022gl099138

Beck, H. E., Zimmermann, N. E., Mcvicar, T. R., Vergopolan, N., Berg, A., & Wood, E. F. (2018). Present and future Koppen-Geiger climate classification maps at 1-km resolution [Dataset]. Scientific Data, *5*, 1–12. https://doi.org/10.1038/sdata.2018.214

Berry, G., Reeder, M. J., & Jakob, C. (2011). A global climatology of atmospheric fronts. *Geophysical Research Letters*, *38*(4), L04809. https://doi.org/10.1029/2010gl046451

Brooks, H. E. (2013). Severe thunderstorms and climate change. *Atmospheric Research*, *123*, 129–138. https://doi.org/10.1016/j.atmosres.2012.04.002

Browning, K. A. (1986). Conceptual models of precipitation systems. *Weather and Forecasting*, *1*(1), 23–41. https://doi.org/10.1175/1520-0434(1986)001<0023:cmops>2.0.co;2

Catto, J. L. (2023). European weather types [Dataset]. https://doi.org/10.24378/exe.4764

Catto, J. L., & Dowdy, A. (2021). Understanding compound hazards from a weather system perspective. *Weather and Climate Extremes*, *32*, 100313. https://doi.org/10.1016/j.wace.2021.100313

Catto, J. L., & Pfahl, S. (2013). The importance of fronts for extreme precipitation. *Journal of Geophysical Research: Atmospheres*, *118*(19), 10791–10801. https://doi.org/10.1002/jgrd.50852

Chen, Y., Liao, Z., Shi, Y., Li, P., & Zhai, P. (2022). Greater flash flood risks from hourly precipitation extremes preconditioned by heatwaves in the Yangtze River Valley. *Geophysical Research Letters*, *49*(18). https://doi.org/10.1029/2022gl099485

CSIRO and Bureau of Meteorology. (2015). Climate change in Australia information for Australia's natural resource management regions: Technical report [Dataset]. Retrieved from https://www.climatechangeinaustralia.gov.au/en/

Dowdy, A., & Brown, A. (2023). Environmental indicators for thunderstorms, lightning and convective rainfall. Bureau Research Report 077. Retrieved from http://www.bom.gov.au/research/publications/researchreports/BRR-077.pdf

Dowdy, A. J. (2020). Climatology of thunderstorms, convective rainfall and dry lightning environments in Australia. *Climate Dynamics*, *54*(5–6), 3041–3052. https://doi.org/10.1007/s00382-020-05167-9

Dowdy, A. J., & Catto, J. L. (2017). Extreme weather caused by concurrent cyclone, front and thunderstorm occurrences. *Scientific Reports*, *7*(1), 40359. https://doi.org/10.1038/srep40359

Dowdy, A. J., Pepler, A., Di Luca, A., Cavicchia, L., Mills, G., Evans, J. P., et al. (2019). Review of Australian east coast low pressure systems and associated extremes. *Climate Dynamics*, *53*(7–8), 4887–4910. https://doi.org/10.1007/s00382-019-04836-8

Fowler, H. J., Lenderink, G., Prein, A. F., Westra, S., Allan, R. P., Ban, N., et al. (2021). Anthropogenic intensification of short-duration rainfall extremes. *Nature Reviews Earth & Environment*, *2*, 107–122. https://doi.org/10.1038/s43017-020-00128-6

Groenemeijer, P. H., & Van Delden, A. (2007). Sounding-derived parameters associated with large hail and tornadoes in the Netherlands. *Atmospheric Research*, *83*(2–4), 473–487. https://doi.org/10.1016/j.atmosres.2005.08.006

Hersbach, H., Bell, B., Berrisford, P., Hirahara, S., Horányi, A., Muñoz-sabater, J., et al. (2020). The ERA5 global reanalysis [Dataset]. Quarterly Journal of the Royal Meteorological Society, *146*(730), 1999–2049. https://doi.org/10.24381/cds.adbb2d47

Hewson, T. D. (1998). Objective fronts. *Meteorological Applications*, *5*(1), 37–65. https://doi.org/10.1017/s1350482798000553

Lavers, D. A., & Villarini, G. (2013). The nexus between atmospheric rivers and extreme precipitation across Europe. *Geophysical Research Letters*, *40*(12), 3259–3264. https://doi.org/10.1002/grl.50636

Leonard, M., Westra, S., Phatak, A., Lambert, M., Van Den Hurk, B., Mcinnes, K., et al. (2014). A compound event framework for understanding extreme impacts. *Wiley Interdisciplinary Reviews-Climate Change*, *5*(1), 113–128. https://doi.org/10.1002/wcc.252

Lewis, E., Fowler, H., Alexander, L., Dunn, R., Mcclean, F., Barbero, R., et al. (2019a). GSDR: A global sub-daily rainfall dataset. *Journal of Climate*, *32*(15), 4715–4729. https://doi.org/10.1175/jcli-d-18-0143.1

Lewis, E., Fowler, H., Alexander, L., Dunn, R., Mcclean, F., Barbero, R., et al. (2019b). Subset of global sub-daily rainfall (GSDR) dataset. https://doi.org/10.5281/ZENODO.8369987

Lewis, E., Pritchard, D., Villalobos-Herrera, R., Blenkinsop, S., Mcclean, F., Guerreiro, S., et al. (2021). Quality control of a global hourly rainfall dataset [Dataset]. Environmental Modelling & Software, *144*, 105169. https://doi.org/10.1016/j.envsoft.2021.105169

Li, C. X., Min, R. Y., Gu, X. H., Gulakhmadov, A., Luo, S. J., Liu, R. H., et al. (2022). Substantial increase in heavy precipitation events preceded by moist heatwaves over China during 1961-2019. *Frontiers in Environmental Science*, *10*. https://doi.org/10.3389/fenvs.2022.951392

Meyer, J., Neuper, M., Mathias, L., Zehe, E., & Pfister, L. (2022). Atmospheric conditions favouring extreme precipitation and flash floods in temperate regions of Europe. *Hydrology and Earth System Sciences*, *26*(23), 6163–6183. https://doi.org/10.5194/hess-26-6163-2022

Miralles, D. G., Gentine, P., Seneviratne, S. I., & Teuling, A. J. (2019). Land-atmospheric feedbacks during droughts and heatwaves: State of the science and current challenges. *Annals of the New York Academy of Sciences*, *1436*(1), 19–35. https://doi.org/10.1111/nyas.13912

Murray, R. J., & Simmonds, I. (1991). A numerical scheme for tracking cyclone centres from digital data. *Australian Meteorological Magazine*, *39*, 155–166.

Ning, G., Luo, M., Zhang, W., Liu, Z., Wang, S., & Gao, T. (2022). Rising risks of compound extreme heat-precipitation events in China. *International Journal of Climatology*, *42*(11), 5785–5795. https://doi.org/10.1002/joc.7561

Pepler, A. S. (2022). Australian weather types, 1979-2015 [Dataset]. figshare. https://doi.org/10.6084/m9.figshare.20335530.v2

Pepler, A. S., Dowdy, A. J., Van Rensch, P., Rudeva, I., Catto, J. L., & Hope, P. (2020). The contributions of fronts, lows and thunderstorms to southern Australian rainfall. *Climate Dynamics*, *55*(5–6), 1489–1505. https://doi.org/10.1007/s00382-020-05338-8

Prein, A. F., Rasmussen, R. M., Ikeda, K., Liu, C., Clark, M. P., & Holland, G. J. (2016). The future intensification of hourly precipitation extremes. *Nature Climate Change*, *7*(1), 48–52. https://doi.org/10.1038/nclimate3168

Púčik, T., Groenemeijer, P., Rýva, D., & Kolář, M. (2015). Proximity soundings of severe and nonsevere thunderstorms in Central Europe. *Monthly Weather Review*, *143*(12), 4805–4821. https://doi.org/10.1175/mwr-d-15-0104.1

Sansom, P. G., & Catto, J. L. (2022). Improved objective identification of meteorological fronts: A case study with ERA-Interim. *Geoscientific Model Development Discussions* [preprint]. https://doi.org/10.5194/gmd-2022-255. (in review).

Sauter, C., Fowler, H. J., Westra, S., Ali, H., Peleg, N., & White, C. J. (2023). Compound extreme hourly rainfall preconditioned by heatwaves most likely in the mid-latitudes. *Weather and Climate Extremes*, *40*, 100563. https://doi.org/10.1016/j.wace.2023.100563

Sauter, C., White, C. J., Fowler, H. J., & Westra, S. (2022). Temporally compounding heatwave-heavy rainfall events in Australia. *International Journal of Climatology*, *43*(2), 1050–1061. https://doi.org/10.1002/joc.7872

Seneviratne, S. I., Zhang, X., Adnan, M., Badi, W., Dereczynski, C., Di Luca, A., et al. (2021). Weather and climate extreme events in a changing climate. In V. Masson-Delmotte, P. Zhai, A. Pirani, S. L. Connors, C. Péan, S. Berger, et al. (Eds.), *Climate change 2021: The physical science basis. Contribution of working group I to the sixth assessment report of the intergovernmental panel on climate change*. Cambridge University Press.

Simmonds, I., & Keay, K. (2000). Mean Southern Hemisphere extratropical cyclone behavior in the 40-year NCEP-NCAR reanalysis. *Journal of Climate*, *13*(5), 873–885. https://doi.org/10.1175/1520-0442(2000)013<0873:mshecb>2.0.co;2

Simmonds, I., Keay, K., & Bye, J. A. T. (2012). Identification and climatology of Southern Hemisphere mobile fronts in a modern reanalysis. *Journal of Climate*, *25*(6), 1945–1962. https://doi.org/10.1175/jcli-d-11-00100.1

Simmonds, I., Murray, R. J., & Leighton, R. M. (1999). A refinement of cyclone tracking methods with data from FROST. *Australian Meteorological Magazine*, 35–49.

Trenberth, K. E., Dai, A., Rasmussen, R. M., & Parsons, D. B. (2003). The changing character of precipitation. *Bulletin of the American Meteorological Society*, *84*(9), 1205–1218. https://doi.org/10.1175/bams-84-9-1205

Villarini, G., & Denniston, R. F. (2016). Contribution of tropical cyclones to extreme rainfall in Australia. *International Journal of Climatology*, *36*(2), 1019–1025. https://doi.org/10.1002/joc.4393

Wernli, H., & Schwierz, C. (2006). Surface cyclones in the ERA-40 dataset (1958-2001). Part I: Novel identification method and global climatology. *Journal of the Atmospheric Sciences*, *63*(10), 2486–2507. https://doi.org/10.1175/jas3766.1

Wu, S. J., Chan, T. O., Zhang, W., Ning, G. C., Wang, P., Tong, X. L., et al. (2021). Increasing compound heat and precipitation extremes elevated by urbanization in South China. *Frontiers in Earth Science*, *9*. https://doi.org/10.3389/feart.2021.636777

You, J., & Wang, S. (2021). Higher probability of occurrence of hotter and shorter heat waves followed by heavy rainfall. *Geophysical Research Letters*, *48*(17), e2021GL094831. https://doi.org/10.1029/2021gl094831

Zhang, W., & Villarini, G. (2020). Deadly compound heat stress-flooding hazard across the Central United States. *Geophysical Research Letters*, *47*(15), e2020GL089185. https://doi.org/10.1029/2020gl089185

Zscheischler, J., Westra, S., Van Den Hurk, B. J. J. M., Seneviratne, S. I., Ward, P. J., Pitman, A., et al. (2018). Future climate risk from compound events. *Nature Climate Change*, *8*(6), 469–477. https://doi.org/10.1038/s41558-018-0156-3